Glyco-platelets with controlled morphologies via crystallization-driven self-assembly and their shape-dependent interplay with macrophages

Li, Zhen; Zhang, Yufei; Wu, Libin; Yu, Wei; Wilks, Thomas; Dove, Andrew; Ding, Hong-ming; O'Reilly, Rachel; Chen, Guosong; Jiang, Ming

DOI:
10.1021/acsmacrolett.9b00221

Glyco-Platelets with Controlled Morphologies via Crystallization-Driven Self-Assembly and their Shape-Dependent Interplay with Macrophages

Zhen Li,[1] Yufei Zhang,[1] Libin Wu,[1] Wei Yu,[2] Andrew P. Dove,[3] Hong-ming Ding,[4*] Rachel K. O'Reilly,[3*] Guosong Chen,[1*] Jiang Ming[1].

[1]The State Key Laboratory of Molecular Engineering of Polymers and Department of Macromolecular Science, Fudan University, Shanghai, 200433, China.

[2]Department of Chemistry, The University of Warwick, Gibbet Hill Road, Coventry, CV4 7AL, United Kingdom.

[3]School of Chemistry, University of Birmingham, Edgbaston, Birmingham B15 2TT, United Kingdom.

[4]Center for Soft Condensed Matter Physics and Interdisciplinary Research, School of Physical Science and Technology, Soochow University, Suzhou 215006, China.

ABSTRACT: Two-dimensional (2D) materials are of great significance to the materials community for their high surface area and controllable surface properties. However, controlled preparation of 2D structures with biological functions and biodegradable features is considerably hard. In this work, we demonstrate that, by careful selection of building block structures and assembly conditions, the above obstacle can be overcome partially by crystallization-driven self-assembly (CDSA) from PLLA-based diblock glycopolymers. 1D glyco-cylinders and 2D diamond-shaped glyco-platelets with solid or hollow core were achieved, where the latter structures have not been reported in literatures so far. The glyco-platelets further demonstrated exciting macrophage activation efficiency with clear size effect compared to their 1D analogues, which indicated their possible potential in immunological applications.

Two-dimensional (2D) planar nanostructures have received extensive attention recently, owing to their distinguished electronic or biomedical properties that originate from their thin and flat morphology.[1-4] Besides the tremendous success in the application of inorganic 2D materials, self-assembly of block copolymers emerges recently as an powerful route to access organic 2D materials.[5, 6] Although block copolymers are well known to prepare core-shell micellar structures including spheres, worm-like micelles, vesicles, preparation of 2D platelets is quite challenging considering the requirement of epitaxial growth of the copolymer and t he followed-up avoidance of surface tension decrease via bending of the lamellas.[7] In recent years, the above difficulty has been partly overcome using the crystallization-driven self-assembly (CDSA) strategy, where crystalline-coil block copolymers favor the formation of micelles with low interfacial curvature as a result of the crystallization of the semi-crystalline segment. The CDSA method has shown to be impressive to access many complex but precisely-defined nanostructures starting from different kinds of semi-crystalline polymers in recent years.[8-16] Although quite a few well-controlled 2D platelet micelles have been reported, most of them were formed in organic solvent, while only in very limited number of cases, water was employed as the bulk solvent with mainly biologically inert blocks e.g. polyethylene glycol as the corona.[17-20] This is mainly ascribed to the lack of synthetic accessibility to bioactive polymers and the tremendous solubility difference between the crystalline block and the bioactive block. Furthermore, water is not friendly to crystallization of many semi-crystalline polymers.[21] Therefore, the CDSA study of block copolymers containing bioactive block in aqueous solution is demanding which could be utilized to fabricate 1D and 2D nanomaterials with biological functionality.

In biological systems, the geometry and surface chemistry of nanoparticles have significant influence in the determination of their interactions with cells and subsequent cellular signaling transduction.[22-24] Our previous study has shown that 1D cylindrical glyconanoparticles induce the inflammatory response of macrophages more efficiently than the spherical glyconanoparticles even with a smaller endocytosis amount.[25] While 2D materials, depending on the size and surface properties, can exhibit unique behaviors in their interactions with cells. For example, graphene-based 2D material have distinctive physical and mechanical bio-interactions modes with cells which are governed by their 2D geometry (shape, thickness, lateral dimension, aspect ratio), surface charge and polarity, and mechanical properties.[4, 26-29] Recently, these graphene-based 2D materials have been used for diverse biological applications

Scheme 1. Synthesis route of PLLA-based diblock glycopolymer.

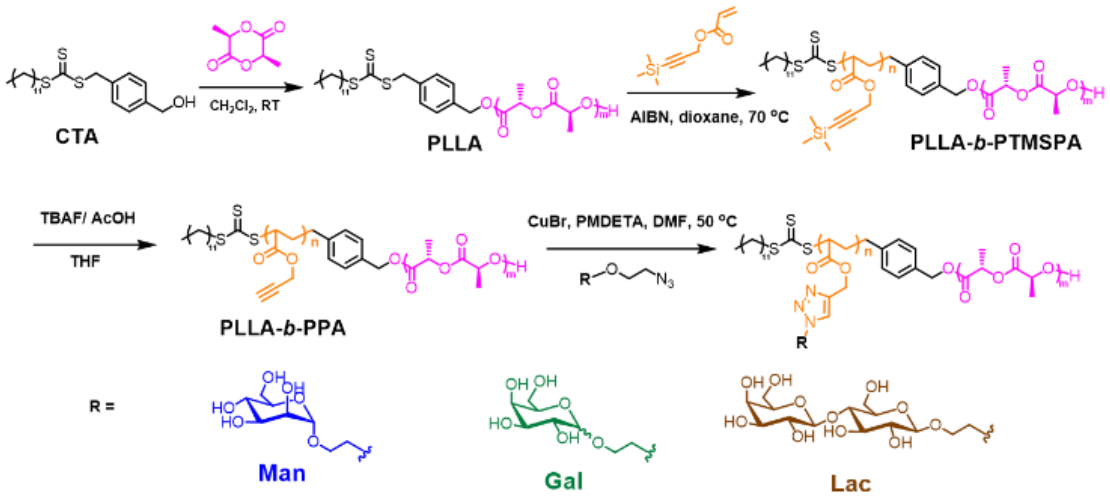

such as stem cell engineering and so on.[30] However, besides the inorganic graphene-based 2D materials, there have been only a small number of reports about organic 2D structures with bioactive functional surfaces,[31, 32] analysis of their structural effect on cellular response is still limited.

Herein, we aim at preparation of polymeric 2D platelet structures in water composed of tailor-made crystalline-coil block copolymers featuring biocompatible poly(L-lactide) (PLLA) as the core-forming block and bioactive carbohydrate block as the hydrophilic part to provide both colloidal stability and surface functionality. Meanwhile, unexpected hollow diamond-shape platelet formation was observed, we attribute that to the mild PLLA degradation. Moreover, the cellular uptake behavior and immunological functions of these glyco-platelets were studied for the first time. It is worth mentioning that the contribution of the glyco-block will be discussed in detail as not only a biocompatible polymer, but a real active block which carbohydrate species could determine the assembly morphology and functionality in the study of immune response.

With a combination of ring opening polymerization (ROP), reversible addition-fragmentation chain transfer (RAFT) polymerization, and Cu(I)-catalyzed azide-alkyne cycloaddition (CuAAC) reaction, we prepared a family of PLLA diblock copolymer amphiphiles (Scheme 1 and Table 1, see Supporting Information for synthesis details). Considering the hydrophobic character of the PLLA block, we first tried conventional solvent-switch method for self-assembly, but this approach usually led to irregular structures with mixed morphology (Figure S22). Then we turned to seek an alternative self-assembly method *i.e.* CDSA technique aiming at uniform structures. Following the success of the assembly preparation in the previous research,[10] polymers in solvent was dissolved as unimers at elevated temperature and as the solution was cooled down, the free polymer chains would undergo homogeneous nucleation and slowly reorganize to form crystalline nanostructures. Notably, in this procedure the solvent should be carefully chosen in which PLLA chains have adequate mobility to crystallize and the coronal block is well-solvated to stabilize the formed nano-objects. We studied the self-assembly of the $PLLA_{33}$-*b*-$PMan_{12}$ in several solvents, namely methanol

Table 1. Characterization of PLLA-based diblock glycopolymer.

Polymer[a]	$Đ_M$ of precursor[b]	M_n (kDa)[a]	Grafting ratio[c]	f_{PLLA} [d]
$PLLA_{33}$-b-$PMan_{12}$	1.15	8.9	88 %	56 %
$PLLA_{33}$-*b*-$PMan_{25}$	1.17	12.7	80 %	39 %
$PLLA_{33}$-*b*-$PGal_{25}$	1.17	12.5	77 %	40 %
$PLLA_{33}$-*b*-$PLac_{25}$	1.17	12.1	43 %	41 %
$PLLA_{44}$-*b*-$PMan_{37}$	1.32	17.3	72 %	37%
$PLLA_{33}$-*b*-$PMan_{62}$	1.28	22.3	68 %	22 %
$PLLA_{33}$-*b*-$PMan_{88}$	1.34	27.6	59 %	18 %

[a] Degree of polymerization (DP) and molecular weight were determined based on the integral result of ^{1}H NMR. [b] Measured by GPC ($CHCl_3$ or THF against polystyrene (PS) standards). [c] Calculated based on the integral result of ^{1}H NMR. [d] PLLA weight fraction in the diblock copolymer.

(MeOH), ethanol (EtOH), water (H_2O), and their mixtures with *N*, *N*-dimethylformamide (DMF). In the cases of EtOH or MeOH, irregular platelet-like structures were found mostly (Figure S23). Although these solvents have been employed in previous PLLA-containing copolymer studies,[10] the bad solubility of the glyco-block resulted in a faster micellization rate of the polymers than its crystallization rate, leading to irregular morphologies. Only when 20 % DMF/ MeOH mixture was employed, some short cylinders were found under TEM (Figure S23f). Glycopolymer is more compatible with water, when we used aqueous solution to do self-assembly, more well-defined structures were obtained. Thus, $PLLA_{33}$-*b*-$PMan_{12}$ was heated in aqueous solution with DMF content varied from 0% to 20% (0.5 mg/mL) at 80 °C for 5 h, then the polymer solution was slowly cooled down to room temperature. As shown in Figure 1a, $PLLA_{33}$-*b*-$PMan_{12}$ assembled in pure water forming jagged cylinders. Interestingly, when a small aliquot of the common solvent DMF was added to the solution before heating, leaf-like platelets were formed, and with more DMF being used, the platelets became larger (Figure 1b, c, d). The number-average area (A_n) increased nearly linearly

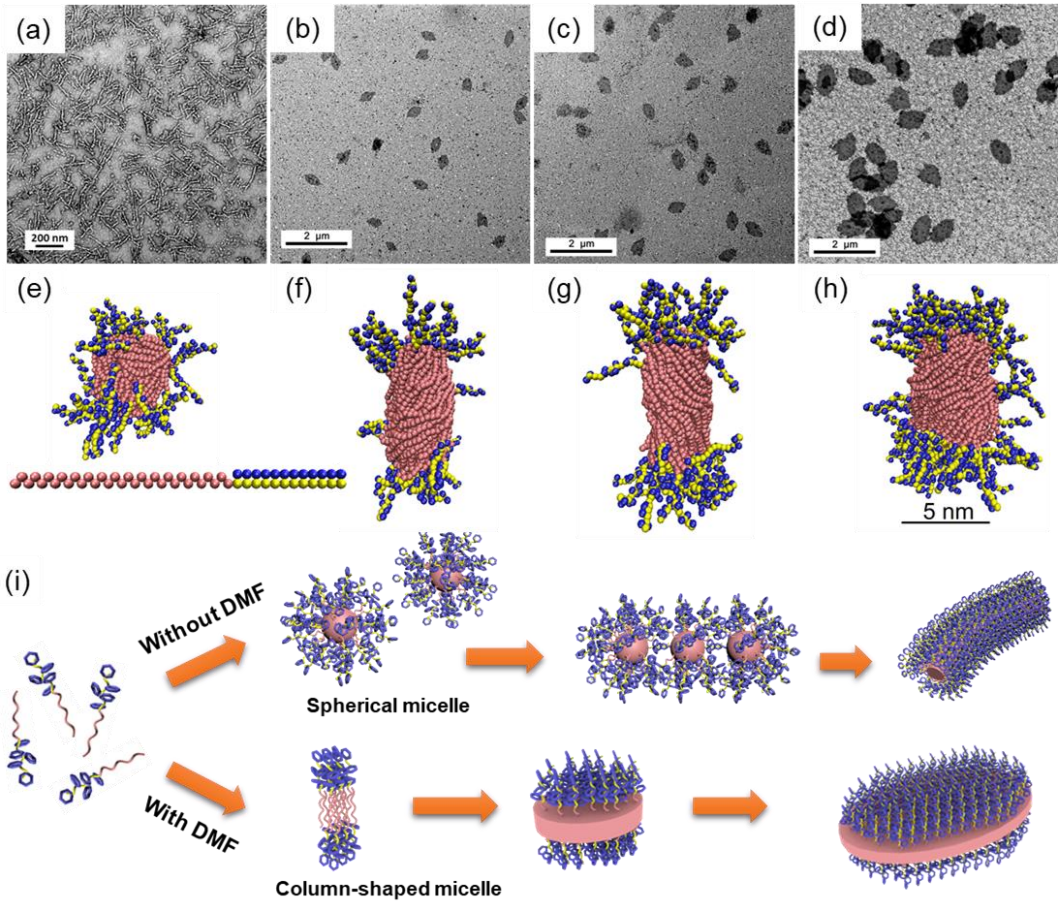

Figure 1. TEM micrographs of $PLLA_{33}$-*b*-$PMan_{12}$ self-assembled in (a) pure H_2O; (b) 5 % DMF/H_2O mixture; (c) 10 % DMF/H_2O mixture; (d) 20% DMF/ H_2O mixture. Polymer solution (0.5 mg/mL) was heated at 80 °C for 5 h and cooled to room temperature. All samples were stained with uranyl acetate. Typical simulation snapshot for the final assembly in different systems: (e) pure H_2O; (f) 5 % DMF/H_2O mixture; (g) 10 % DMF/H_2O mixture; (h) 20% DMF/ H_2O mixture. (i) Schematic illustration of CDSA process of $PLLA_{33}$-*b*-$PMan_{12}$ diblock copolymers in aqueous solutions with/without DMF.

from 1.1×10^5 nm² to 3.1×10^5 nm² when the DMF ratio increased from 5% to 20% (Table S1). However, the thickness of all these platelets kept uniform, were about 10 nm, (Figure S24) typical of a polymer crystal with a single layer of chain folds. [33, 34]These results can be rationalized by the crystallization characteristics of the PLLA core-forming block, where DMF acted as a "plasticizer" to increase the solubility of the crystallizable PLLA core-forming block and facilitated the crystallization,[35]. Such an apparent morphology change was hardly seen in other aqueous CDSA systems without glycopolymers.

To provide more physical insights into the DMF-ratio-dependent morphology in the experiments, dissipative particle dynamics (DPD) simulations (see details of DPD method in SI) were employed to investigate the self-assembly of glycopolymers at the molecular level. The modeling of $PLLA_{33}$-*b*-$PMan_{12}$ was established by using the coarse-grained (CG) method, where each group in the polymers was represented by using one CG bead in the simulation (see the inset of Fig. 1e and Figure S25). The self-assembly behavior in pure water was firstly investigated. As shown in Figure S26a, hundreds of $PLLA_{33}$-*b*-$PMan_{12}$ were randomly placed in the solvated simulation box at the beginning. Due to the hydrophobicity of the PLLA (i.e., strong PLLA-PLLA interaction in H_2O), the polymers quickly formed into small aggregates. As time went on, the small aggregates fused and changed into spherical micelles, with the PLLA as the core and the glyco-block as the corona to minimize the undesired contact between PLLA and H_2O. And such structure remained stable until the end of the simulation. In the presence of DMF, the polymers also aggregated with each other and then fused into spherical micelles (Fig. S26b), which was similar to that in the case of pure H_2O. Nevertheless, as time went on (i.e., the temperature decreased), there existed an obvious shape transition, *i.e.*, from the spherical to the column-shaped micelle (the glyco-block mainly distributed at the two ends of the micelle). Due to the addition of DMF into H_2O, the incompatibility of PLLA parts with the solvent became weak. In addition, the conformational entropy of the PLLA parts at low temperature was also decreased, thus the PLLA could be stretched (to enhance PLLA-PLLA interaction) under this situation.

In general, the DPD simulation showed that the addition of DMF (to H_2O) can induce the shape transition of micelles. Such difference can be enlarged by further packing of these micelles. As shown Figure 1i, the spherical micelles could be just packed in one direction due to the protection of glyco-block, while the column-shaped micelles were able to grow in a two-dimensional manner and finally formed the 2D structure. Notably, the size of the spherical micelle and the height of the column-shaped micelle in the simulation was about 10 nm (Figure 1e-h), in good agreement with the diameter of the jagged cylinder and the height of the platelet (in the experiment), respectively. These results further confirmed the rationality of the proposed mechanism.

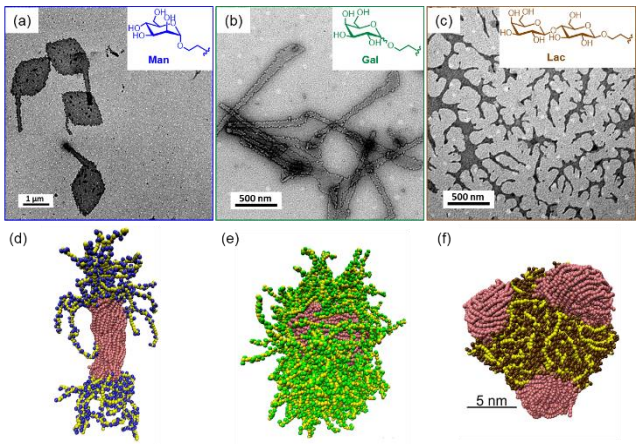

Figure 2. Different CDSA morphologies of PLLA containing diblock copolymers caused by different carbohydrate compositions: (a) $PLLA_{33}$-*b*-$PMan_{25}$, (b) $PLLA_{33}$-*b*-$PGal_{25}$, (c) $PLLA_{33}$-*b*-$PLac_{25}$ self-assembled in 5% DMF/H_2O mixture. Polymer solution (0.5 mg/mL) was heated at 80 °C for 5 h and cooled to room temperature. All samples were stained with uranyl acetate. Typical simulation snapshot for the final assembly in different systems: (d) $PLLA_{33}$-*b*-$PMan_{25}$, (e) $PLLA_{33}$-*b*-$PGal_{25}$, (f) $PLLA_{33}$-*b*-$PLac_{25}$.

In nature, cells have various types of carbohydrates superficial to the membrane and these carbohydrate species are closely associated with cellular functions. To mimic this kind of structure, we intend to study the CDSA of diblock copolymer with different kinds of saccharides. With the same polymer precursor $PLLA_{33}$-*b*-PPA_{25}, the impact from the attached carbohydrate type on the final morphology were explored. As shown in Figure 2, mannoside-conjugated polymer $PLLA_{33}$-*b*-$PMan_{25}$ self-assembled into diamond with a tail shape morphology, indicating that maybe the transitional copolymer composition from cylinder to platelet has been reached. The process could be rationalized as that platelets were formed at initial stage, then the remaining polymers underwent an epitaxial growth on the edge of the platelet to form elongated structures. However, when galactoside, one of the stereoisomers of mannoside, was used and the copolymers had the same backbone and very similar grafting ratio, we found that the resultant morphology was totally different, i.e. stick-like structure became favored. In contrast, when lactoside was employed with similar carbohydrate content, ill-defined platelets were formed, similar to CDSA behaviors of $PLLA_{33}$-*b*-$Pman_{12}$ in EtOH or MeOH (Figure S23). To understand the distinct self-assembly behavior of the polymers containing different types of carbohydrates, DPD simulation was again employed. Similar to $PLLA_{33}$-*b*-$PMan_{12}$, here the final assembly of $PLLA_{33}$-*b*-$PMan_{25}$ was also the column-shaped micelle (Figure 2d), thus (after further packing) the platelets could be observed in the experiments. While for $PLLA_{33}$-*b*-$PGal_{12}$, due to the poorer solubility of galactose and weaker carbohydrate-carbohydrate interactions,[36] the final assembly in the simulation was sphere-like structures (Figure 2e and Figure S27). These structures are with more crowded glyco-corona and less PLLA exposure in the middle region. Then they could not grow in all directions on the plane to form a platelet, instead they may grow in one favored direction and further pack into the stick-like structure, similar to previous case of $PLLA_{33}$-*b*-$PMan_{12}$ without DMF (the upper illustration in Figure 1i). When the type of carbohydrate changed to lactose, the very poor solubility of lactose led to the irregular assembly --- the PLLA and the glyco-block just separated with each other (Figure 3f and Figure 27b). Since here the glyco-block cannot be used to protect the undesired contact between PLLA and H_2O, no micelle-like structure could be formed (in the simulation), which may give some hint for the ill-defined aggregates in the experiments.

Previous self-assembled $PLLA_{33}$-*b*-$Pman_{12}$ platelets have a rather rugged edge and are not lozenge-shaped like polymer single crystal, but when the polymer with a longer PLLA block and larger hydrophilic ratio, e.g. $PLLA_{44}$-*b*-$Pman_{37}$, was employed, smooth-edged diamond-shaped platelets were formed in μm scale (Figure 3a). The result indicated that in this system a longer PLLA would lead to more perfect crystallization than the shorter one. The crystalline nature of the diamond-shaped platelets was further confirmed by the wide-angle X-ray diffraction (WAXD) analysis (Figure S28). The strongest peak at 16.8° comes from the diffraction of (110)/(200) planes and the peak at 19.2° comes from (203).[36] Unexpectedly, when the solvent temperature was increased to 90 °C with extended heating time to 8 h, hollow diamonds were found (Figure 3b). After dialysis against water to remove DMF, the solid/hollow 2D glyconanoparticles were still colloidally stable with carbohydrates covered on the micelle surface (Figure S29). Moreover, FITC-ConA (lectins specifically binding to mannose), or gold nanoparticles were able to be selectively label the 2D platelets as shown in Figure S30 as a consequence of their specialized interactions with the platelet corona.

In literatures, fabrication of hollow platelet structure was seldom reported and demanded multiple steps: stagewise growth of patchy platelet, crosslinking of the peripheral section and dissolution of the central uncross-linked region.[6, 37] Obviously the current attractive formation of the hollow diamond-shaped platelet needs no complicated and laborious steps and seems promising. We tried different other polymers to follow the same process (90 °C, 8h, 10% DMF) hoping to realize the hollow platelet morphology. We found that longer polymer $PLLA_{33}$-*b*-$PMan_{62}$ and

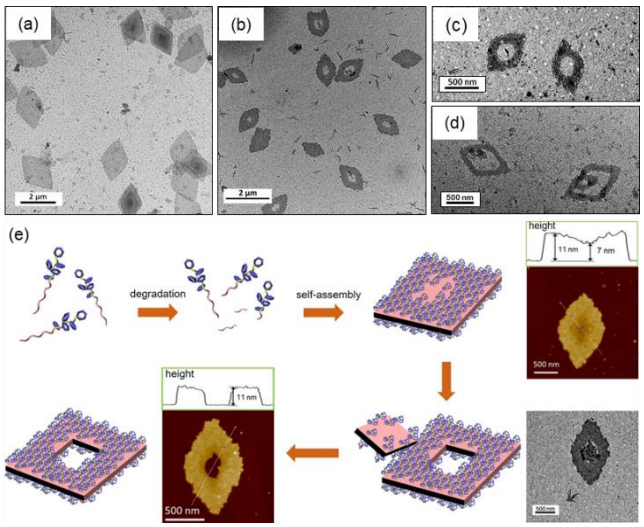

Figure 3. TEM micrographs of block copolymer self-assembled in 5 % DMF:/H_2O mixture: (a) $PLLA_{44}$-*b*-$Pman_{37}$ was heated at 80 °C for 5 h, (b) $PLLA_{44}$-*b*-$Pman_{37}$ was heated at 90 °C for 8 h, (c) $PLLA_{33}$-*b*-$Pman_{62}$ was heated at 90 °C for 8 h, (d) $PLLA_{33}$-*b*-$Pman_{88}$ was heated at 90 °C for 8 h before cooling to room temperature. All samples were stained with uranyl acetate. (e) Proposed formation mechanism of hollow diamond-shaped platelet and captured intermediate states using AFM and TEM.

.

$PLLA_{33}$-*b*-$PMan_{88}$ can easily form similar hollow platelet like $PLLA_{44}$-*b*-$Pman_{37}$ polymer (Figure 3c, 3d), but shorter $PLLA_{33}$-*b*-$PMan_{12}$ and $PLLA_{33}$-*b*-$PMan_{25}$ polymer cannot form hollow platelet. However, when we increase the DMF ratio in solution, they can form hollow platelet too (for PLLA33-b-Pman12, 50 %DMF; for PLLA33-Pman25, 20 % DMF, Figure S31). We further checked the chemical composition change of the $PLLA_{44}$-*b*-$Pman_{37}$ hollow diamond sample. We found that some block copolymer degraded weakly after a long-time heating process at elevated temperature, the degraded product can be consolidated by ^{1}H NMR (Figure S32). Specifically, peak intensity of the doublet at δ 5.21 ppm and the quartet at δ 1.47 ppm attributed to CH group and CH_3 group from PLLA decreased and the doublet at δ 4.04 ppm and the quartet at δ 1.14 ppm assigned to the degraded products of the PLLA segments appeared. DOSY spectra also told that after long time heating, molecules with larger diffusion coefficient at chemical shifts of δ 4.04 ppm and δ 1.14 ppm appeared (Figure S33).

Combining that, we found that there are two parameters determining the hollow platelet formation: (a) the high polydispersity of the block glycopolymer which was caused by weak degradation after long-time heating at elevated temperature; (b) the adequate mobility of polymer chain in solution/platelet which was associated with the DMF ratio in solution and glyco-block length of the polymer. With bigger DMF ratio or longer glyco-block, the polymer chain would have better mobility. The high polydispersity of the block copolymer allows the apparent chemical composition difference between central region and the outer region in the platelet, and the adequate mobility of polymer chain would make the central small platelet exfoliating from the big platelet possible.

As shown in Figure 3e, we give a possible hollow platelet forming mechanism. After long time heating, the resulted shortened block copolymers might crystallize first as nuclei and pristine PLLA-*b*-Pman block copolymers add into the diamond next. This hypothesis was confirmed by AFM imaging. Unlike the solid diamond formed at low heating temperature (Figure S34), AFM images of diamonds formed with a longer heating time (Figure 4e, top right) show a concave surface structure with a height in the central region lower than that in the outer region. And because the central region of the diamond has less glycopolymer to maintain its stability than the outer region, it tends to slip from the diamond, and this slipping process was also captured by the TEM analysis (Figure 4e, bottom right). On the other hand, the degradation leads to change of the polymer composition, some polymers favor cylinder, which makes some cylinders existing near the hollow diamond understandable (Figure 3b). When we added trace of mild base into the system to slightly promote the PLLA degradation but did not cause its full degradation, nearly pure cylinders were found from the TEM (Figure S35).

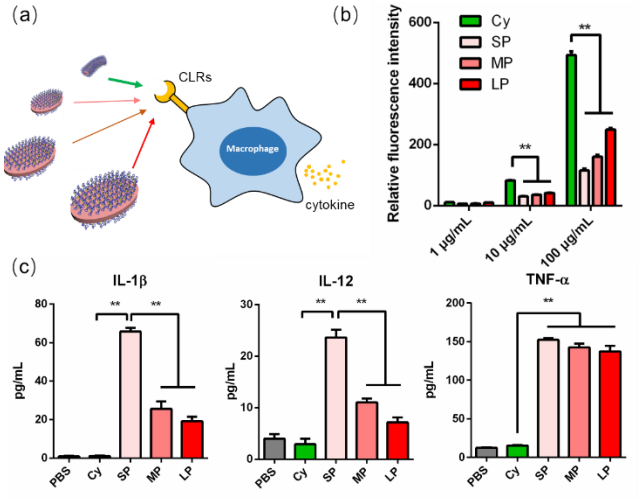

Figure 4. (a) Schematic illustration of different glyconanoparticles interacting with macrophages. (b) Dose-dependent endocytosis of different fluorescent $PLLA_{33}$-*b*-$Pman_{12}$ glyconanoparticles by RAW264.7 macrophages. (c) Glyconanoparticles with different size/shape (10 μg/mL) promoted the IL-1β, IL-12, TNF-α, secretions of macrophages after 24 h incubation measured by ELISA. Data are expressed as the mean ± SEM of three independent experiments; *p < 0.05 and **p < 0.01. Cy: cylinder, SP: small platelet, MP: medium platelet, LP: large platelet.

We have demonstrated that PLLA-based glycopolymer could be used to fabricate two-dimensional glyco-platelet, then we tried to studied their interactions with cells. The above obtained glyconanoparticles formed by $PLLA_{33}$-*b*-$Pman_{12}$ polymer are with well-controlled shape and size are ideal for further biological study. Therefore, *via* co-assembly of fluorescent $PLLA_{33}$-*b*-$Pmancya_{25}$ polymer (synthesis details were given in Supporting Information) with $PLLA_{33}$-*b*-$Pman_{12}$, we obtained four kinds of glyconanoparticles, i.e. cylinders (Cy), small platelets (SP), medium platelets (MP)

and large platelets (LP) which were labeled with fluorescence without big change of glyconanoparticles shape and size. The residual DMF was removed by dialysis against water, and the size of these glyconanoparticles was summarized in supporting information. (Figure S25, Table S2). Before cellular study, the biocompatibility of these glyconanoparticles was first confirmed through cell viability assays, which showed negligible cytotoxicity up to 100 μg/mL (Figure S26). It was found that the shape of the glyconanoparticles has a strong influence on its cellular uptake behaviors: 1D glyco-cylinders have obvious higher uptake efficiency than 2D glyco-platelets. Meanwhile, the size has a moderate effect on the cellular uptake, i.e. the LPs were internalized slightly more than the SPs (Figure 4b). We further used the four kinds of glyconanoparticles with different morphologies to study their immune stimulating properties by measuring the cytokine release after incubation with RAW264.7 macrophages. Six different proinflammatory cytokines IL-1β, IL-12, TNF-α, IL-6, IL-10, CCL-2 were evaluated after incubating these glyconanoparticles with RAW264.7 macrophages. Compared with cylinders, all three kinds of glyco-platelets showed stronger stimulated secretion of the pro-inflammatory cytokines, and the small glycoplatelets induced stronger cytokine release than the bigger ones (Figure 4c, Figure S27). Interestingly, the endocytosis experiment just showed an opposite trend compared with the cytokine release behaviors. It seems that the morphology plays a crucial role in this process, and the platelet-shaped glyconanoparticles are more efficient in macrophage activation than the cylinder-shaped ones, even with smaller number of particles being uptake.

In conclusion, we demonstrated a simple method using the CDSA of diblock glycopolymer to form different carbohydrate-functionalized platelets. Furthermore, we observed a morphological transition to form hollow platelets utilizing the degradation property of the PLLA block on heating in solution. We further move forward by employing these materials for biological study. It was found that the glyconanoparticles of different size and morphology showed different ability to induce the inflammatory response. Platelet-like glyconanoparticles induce the inflammatory response more efficiently than cylinder-like ones and smaller glyco-platelets demonstrated higher stimulating efficiency. The choice of platelet with optimized size opens a new avenue to construct biodegradable immune stimulating materials, which might be useful to convert immunoseppressive tumor microenvironment in cancer immunotheapy.

ASSOCIATED CONTENT

Supporting Information.
The Supporting Information is available free of charge on the ACS Publications website at DOI: ######.

Materials and methods, characterization, and supporting figures and table (PDF)

AUTHOR INFORMATION

Corresponding Author

* guosong@fudan.edu.cn (GC)
* r.oreilly@bham.ac.uk (ROR)
* dinghm@suda.edu.cn (HD)

ORCID

Guosong Chen: 0000-0001-7089-911X
Rachel K. O'Reilly: 0000-0002-1043-7172
Hong-ming Ding: 0000-0002-9224-4779

Notes

The authors declare no competing financial interest.

ACKNOWLEDGMENT

G.C. thanks NSFC/China (No. 51721002, 21861132012 and 91527305). H.M.D thanks NSFC/China (No. 21604060).

REFERENCES

(1) Zhuang, X.; Mai, Y.; Wu, D.; Zhang, F.; Feng, X., Two-Dimensional Soft Nanomaterials: A Fascinating World of Materials. *Adv. Mater.* **2015,** 27 (3), 403-427.
(2) Boott, C. E.; Nazemi, A.; Manners, I., Synthetic Covalent and Non-Covalent 2D Materials. *Angew. Chem. Int. Ed.* **2015,** 54 (47), 13876-13894.
(3) Tan, C.; Cao, X.; Wu, X.; He, Q.; Yang, J.; Zhang, X.; Chen, J.; Zhao, W.; Han, S.; Nam, G.; Sindoro, M.; Zhang, H., Recent Advances in Ultrathin Two-Dimensional Nanomaterials. *Chem. Rev.* **2017,** 117 (9), 6225-6331.
(4) Wang, Z.; Zhu, W.; Qiu, Y.; Yi, X.; von Dem, B. A.; Kane, A.; Gao, H.; Koski, K.; Hurt, R., Biological and environmental interactions of emerging two-dimensional nanomaterials. *Chem. Soc. Rev.* **2016,** 45 (6), 1750-80.
(5) Hudson, Z. M.; Boott, C. E.; Robinson, M. E.; Rupar, P. A.; Winnik, M. A.; Manners, I., Tailored hierarchical micelle architectures using living crystallization-driven self-assembly in two dimensions. *Nat. Chem.* **2014,** 6 (10), 893-898.
(6) Qiu, H.; Gao, Y.; Boott, C. E.; Gould, O. E. C.; Harniman, R. L.; Miles, M. J.; Webb, S. E. D.; Winnik, M. A.; Manners, I., Uniform patchy and hollow rectangular platelet micelles from crystallizable polymer blends. *Science* **2016,** 352 (6286), 697-701.
(7) Mai, Y.; Eisenberg, A., Self-assembly of block copolymers. *Chem. Soc. Rev.* **2012,** 41 (18), 5969-5985.
(8) Gilroy, J. B.; Gädt, T.; Whittell, G. R.; Chabanne, L.; Mitchels, J. M.; Richardson, R. M.; Winnik, M. A.; Manners, I., Monodisperse cylindrical micelles by crystallization-driven living self-assembly. *Nat. Chem.* **2010,** 2 (7), 566-570.
(9) Qiu, H.; Hudson, Z. M.; Winnik, M. A.; Manners, I., Multidimensional hierarchical self-assembly of amphiphilic cylindrical block comicelles. *Science* **2015,** 347 (6228), 1329-1332.
(10) Maria, I.; Graeme, C.; Anais, P.; Zachary, P. L. L.; Neil, R. W.; Robert, T. M.; Dove, A. P.; O'Reilly, R. K., 1D vs. 2D shape selectivity in the crystallization-driven self-assembly of polylactide block copolymers. *Chem. Sci.* **2017,** 8, 4423-4230.
(11) Arno, M. C.; Inam, M.; Coe, Z.; Cambridge, G.; Macdougall, L. J.; Keogh, R.; Dove, A. P.; O Reilly, R. K., Precision Epitaxy for Aqueous 1D and 2D Poly(ε -caprolactone) Assemblies. *J. Am. Chem. Soc.* **2017,** 139 (46), 16980-16985.
(12) Rizis, G.; van de Ven, T. G. M.; Eisenberg, A., Crystallinity-driven morphological ripening processes for poly(ethylene oxide)-block-polycaprolactone micelles in water. *Soft Matter* **2014,** 10 (16), 2825.
(13) Schmelz, J.; Karg, M.; Hellweg, T.; Schmalz, H., General Pathway toward Crystalline-Core Micelles with Tunable Morphology and Corona Segregation. *ACS Nano* **2011,** 5 (12), 9523-9534.
(14) Brubaker, C. E.; Velluto, D.; Demurtas, D.; Phelps, E. A.; Hubbell, J. A., Crystalline Oligo(ethylene sulfide) Domains Define

Highly Stable Supramolecular Block Copolymer Assemblies. *ACS Nano* **2015,** 9 (7), 6872-6881.

(15) Fan, B.; Wang, R.; Wang, X.; Xu, J.; Du, B.; Fan, Z., Crystallization-Driven Co-Assembly of Micrometric Polymer Hybrid Single Crystals and Nanometric Crystalline Micelles. *Macromolecules* **2017,** 50 (5), 2006-2015.

(16) Qian, J.; Li, X.; Lunn, D. J.; Gwyther, J.; Hudson, Z. M.; Kynaston, E.; Rupar, P. A.; Winnik, M. A.; Manners, I., Uniform, High Aspect Ratio Fiber-like Micelles and Block Co-micelles with a Crystalline π-Conjugated Polythiophene Core by Self-Seeding. *J. Am. Chem. Soc.* **2014,** 136 (11), 4121-4124.

(17) Rizis, G.; van de Ven, T. G. M.; Eisenberg, A., "Raft" Formation by Two-Dimensional Self-Assembly of Block Copolymer Rod Micelles in Aqueous Solution. *Angew. Chem. Int. Ed.* **2014,** 53 (34), 9000-9003.

(18) Wang, J.; Zhu, W.; Peng, B.; Chen, Y., A facile way to prepare crystalline platelets of block copolymers by crystallization-driven self-assembly. *Polymer* **2013,** 54 (25), 6760-6767.

(19) Su, M.; Huang, H.; Ma, X.; Wang, Q.; Su, Z., Poly(2-vinylpyridine)-block-Poly(ϵ -caprolactone) Single Crystals in Micellar Solution. *Macromol. Rapid. Comm.* **2013,** 34 (13), 1067-1071.

(20) Ganda, S.; Dulle, M.; Drechsler, M.; Förster, B.; Förster, S.; Stenzel, M. H., Two-Dimensional Self-Assembled Structures of Highly Ordered Bioactive Crystalline-Based Block Copolymers. *Macromolecules* **2017,** 50 (21), 8544-8553.

(21) Nazemi, A.; Boott, C. E.; Lunn, D. J.; Gwyther, J.; Hayward, D. W.; Richardson, R. M.; Winnik, M. A.; Manners, I., Monodisperse Cylindrical Micelles and Block Comicelles of Controlled Length in Aqueous Media. *J. Am. Chem. Soc.* **2016,** 138, (13), 4484-4493.

(22) Zhang, S.; Gao, H.; Bao, G., Physical Principles of Nanoparticle Cellular Endocytosis. *ACS Nano* **2015,** 9 (9), 8655-8671.

(23) Verma, A.; Stellacci, F., Effect of surface properties on nanoparticle-cell interactions. *Small* **2010,** 6 (1), 12-21.

(24) Chen, X.; Yan, Y.; Müllner, M.; Ping, Y.; Cui, J.; Kempe, K.; Cortez-Jugo, C.; Caruso, F., Shape-Dependent Activation of Cytokine Secretion by Polymer Capsules in Human Monocyte-Derived Macrophages. *Biomacromolecules* **2016,** 17 (3), 1205-1212.

(25) Li, Z.; Sun, L.; Zhang, Y.; Dove, A. P.; O Reilly, R. K.; Chen, G., Shape Effect of Glyco-Nanoparticles on Macrophage Cellular Uptake and Immune Response. *ACS Macro Lett.* **2016,** 5 (9), 1059-1064.

(26) Titov, A. V.; Král, P.; Pearson, R., Sandwiched Graphene–Membrane Superstructures. *ACS Nano* **2010,** 4 (1), 229-234.

(27) Tu, Y.; Lv, M.; Xiu, P.; Huynh, T.; Zhang, M.; Castelli, M.; Liu, Z.; Huang, Q.; Fan, C.; Fang, H.; Zhou, R., Destructive extraction of phospholipids from Escherichia coli membranes by graphene nanosheets. *Nat. Nanotechnol.* **2013,** 8 (8), 594-601.

(28) Li, Y.; Yuan, H.; von Dem Bussche, A.; Creighton, M.; Hurt, R. H.; Kane, A. B.; Gao, H., Graphene microsheets enter cells through spontaneous membrane penetration at edge asperities and corner sites. *Proc. Natl. Acad. of Sci. U. S. A.* **2013,** 110 (30), 12295-12300.

(29) Yi, X.; Gao, H., Cell interaction with graphene microsheets: near-orthogonal cutting versus parallel attachment. *Nanoscale* **2015,** 7 (12), 5457-5467.

(30) Cheng, C.; Li, S.; Thomas, A.; Kotov, N. A.; Haag, R., Functional Graphene Nanomaterials Based Architectures: Biointeractions, Fabrications, and Emerging Biological Applications. *Chem. Rev.* **2017,** 117 (3), 1826-1914.

(31) Qi, Z.; Bharate, P.; Lai, C.; Ziem, B.; Böttcher, C.; Schulz, A.; Beckert, F.; Hatting, B.; Mülhaupt, R.; Seeberger, P. H.; Haag, R., Multivalency at Interfaces: Supramolecular Carbohydrate-Functionalized Graphene Derivatives for Bacterial Capture, Release, and Disinfection. *Nano Lett.* **2015,** 15 (9), 6051-6057.

(32) Dai, B.; Li, D.; Xi, W.; Luo, F.; Zhang, X.; Zou, M.; Cao, M.; Hu, J.; Wang, W.; Wei, G.; Zhang, Y.; Liu, C., Tunable assembly of amyloid-forming peptides into nanosheets as a retrovirus carrier. *Proc. Natl. Acad. of Sci. U. S. A* **2015,** 112 (10), 2996-3001.

(33) Wang, Z.; Cao, Y.; Song, J.; Xie, Z.; Wang, Y., Cooperation of Amphiphilicity and Crystallization for Regulating the Self-Assembly of Poly (ethylene glycol)-block-poly (lactic acid) Copolymers. *Langmuir* **2016,** 32 (37), 9633-9639.

(34) Fu, J.; Luan, B.; Yu, X.; Cong, Y.; Li, J.; Pan, C.; Han, Y.; Yang, Y.; Li, B., Self-Assembly of Crystalline-Coil Diblock Copolymer in Solvents with Varying Selectivity: From Spinodal-like Aggregates to Spheres, Cylinders, and Lamellae. *Macromolecules* **2004,** 37 (3), 976-986.

(35) Hsiao, M.; Yusoff, S. F. M.; Winnik, M. A.; Manners, I., Crystallization-Driven Self-Assembly of Block Copolymers with a Short Crystallizable Core-Forming Segment: Controlling Micelle Morphology through the Influence of Molar Mass and Solvent Selectivity. *Macromolecules* **2014,** 47 (7), 2361-2372.

(36) Pan, P.; Kai, W.; Zhu, B.; Dong, T.; Inoue, Y., Polymorphous Crystallization and Multiple Melting Behavior of Poly(L-lactide): Molecular Weight Dependence. *Macromolecules* **2007,** 40 (19), 6898-6905.

(37) He, X.; He, Y.; Hsiao, M.; Harniman, R. L.; Pearce, S.; Winnik, M. A.; Manners, I., Complex and Hierarchical 2D Assemblies via Crystallization-Driven Self-Assembly of Poly(L-lactide) Homopolymers with Charged Termini. *J. Am. Chem. Soc.* **2017,** 139, (27), 9221-9228.

Insert Table of Contents artwork here